Heliyon 9 (2023) e19900

Contents lists available at ScienceDirect

Heliyon

journal homepage: www.cell.com/heliyon

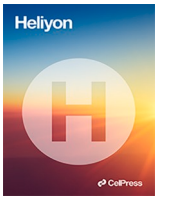

Assessing and improving active travel around urban hospitals: A case of Xiangya hospital, China

Haoyu Deng, Tao Wang *

Beijing Institute of Technology, Beijing, 102488, China

ARTICLE INFO

Keywords:
Extenics
COVID-19
Urban planning
Active travel
Hospital

ABSTRACT

Since the outbreak of COVID-19, there has been a growing trend toward active travel. However, many cities have not given sufficient attention to active transportation, resulting in inadequate safety measures for pedestrians and cyclists. This issue becomes particularly critical around hospitals, closely associated with COVID-19 and where traffic can be more intricate and hazardous. Hence, there is a pressing need for a quantitative assessment of the active travel environment surrounding hospitals to obtain a practical evaluation and devise improvement strategies. This study constructs an Extenics evaluation model to assess the safety, accessibility, traffic pressure, convenience, and comfort of the active travel environment near Xiangya Hospital. Subsequently, optimization strategies are proposed based on the evaluation outcomes. The evaluation results show high traffic pressure around the hospital during peak hours while the infrastructure is insufficient. A diversion strategy must be developed based on the evaluation findings to address safety concerns. Furthermore, issues such as inadequate non-motorized lanes and accessibility facilities in the area are identified. Correspondingly, improvement strategies tailored to the specific problems of each street are suggested based on the evaluation results. While this research focuses on urban hospitals, it aims to offer valuable insights into evaluating and enhancing active travel environments around large public buildings.

1. Introduction

Active travel, including pedestrian and non-motorized modes of transportation, is gaining popularity as a means of short-distance travel and connecting with transit options in modern transportation systems [1]. Besides mitigating urban air pollution, active travel offers significant health advantages by lowering the risk of diseases associated with sedentary lifestyles [2]. Consequently, numerous cities are now recognizing the pivotal role of active travel and its associated benefits [3].

During COVID-19, a significant shift in travel behavior occurred as individuals tended to minimize social contact. Car usage declined while cycling experienced a resurgence, leading to an increased propensity for utilizing active travel for commuting [4,5]. A study revealed that 40–60% of respondents in major cities across the United States, China, and Western Europe expressed their intention to reduce the use of public transportation during the lockdown. Additionally, there was a notable rise in adopting bicycles and shared bikes in the United States and China [6]. The reduction in travel during the lockdown decreased overall traffic-related casualties, particularly minor or non-fatal injuries. However, no significant decrease in serious or fatal injuries. Notably, during COVID-19, the average number of bicyclists who died or were injured per crash more than tripled in New York City compared to the

* Corresponding author.
E-mail address: wangtao1020@126.com (T. Wang).

https://doi.org/10.1016/j.heliyon.2023.e19900
Received 21 April 2023; Received in revised form 4 September 2023; Accepted 5 September 2023
Available online 9 September 2023

same period in previous years [7,8]. Furthermore, the lockdown harmed e-bike safety in some Chinese provinces [9].

The increasing popularity of active travel has highlighted the issue of roads prioritizing the needs of cars. A recent investigation uncovered common deficiencies in sidewalk conditions and the absence of bicycle lanes as contributing factors to active travel casualty hotspots in Ahmedabad [10]. Car-oriented roads often exhibit inadequate space allocation for active travel, including narrow bike lanes or sidewalks and insufficient infrastructure [11,12]. Consequently, pedestrians and cyclists face inconvenience and encounter safety hazards. However, providing safe infrastructure can mitigate car risks to cyclists [13,14]. The odds of injury per kilometer on roads with bicycle lanes are one in nine on major roads without bicycle infrastructure [15].

Insufficient parking capacity is a prevalent issue in certain large hospitals in China. Limited parking spaces in central Shanghai hospitals result in prolonged waiting times for cars, leading to traffic congestion. Consequently, many vehicles park illegally on the roadside or intrude on the sidewalk, contributing to traffic mixing [16]. A case study conducted in Nanjing demonstrated that on-road parking encourages bicycles to navigate on motorways [17]. Furthermore, hospitals implemented a closed-loop management system and pre-screening and triage procedures at their entrances during the lockdown. Only a designated entrance for patients and staff remained open, while individuals seeking admission to the hospital had to undergo information verification [18]. Additionally, to make it easier for people who need to get a NAT, there usually is a detection site around the hospital [19]. These measures concentrate traffic flow, which, combined with inadequate parking spaces and inadequate facilities, heightens risks associated with active travel around the hospital. However, addressing such issues by widening roads or building a parking lot is often unfeasible due to hospitals' urban center locations. Therefore, it is essential to evaluate the capacity of each road to handle peak traffic flow and propose appropriate adjustment strategies.

To devise a sound strategy, analyzing the existing traffic conditions is necessary. Quantitative evaluation offers a logical, standardized, and precise approach. It enables the examination of cause-and-effect relationships among various phenomena, thereby facilitating deriving conclusions. These conclusions, in turn, serve as valuable guidance for strategy development.

Presently, the main quantitative evaluation systems for active travel environments primarily concentrate on the quality of equipment and facilities. Teng et al. introduced an evaluation framework from two key aspects: facility and operation, to assess the hardware components within the active transportation network in Jiawang District, Xuzhou City, Jiangsu Province [20]. Their focus is ensuring safety. Jin Jun et al. evaluated the effectiveness of connectivity, physical and psychological comfort to examine the quality of walking environments in commercial centers [21]. Their research narrowed the scope from city-wide evaluation to building complex areas, emphasizing walking environment comfort and transportation convenience. Guo et al. quantitatively investigated pedestrian transportation systems, considering aspects such as space, interface, and facility comfort [22]. Their study specifically targeted a residential community and emphasized the pedestrian experience. However, there is a lack of research focusing on the surroundings of large public buildings such as hospitals. Since large public buildings may influence surrounding traffic, impacting traffic safety and improvement strategies, existing evaluation metrics may not meet demand.

In evaluation tools, the commonly applied methods in current research include the TOPSIS and DEA. Yan combined entropy power with TOPSIS analysis methods to construct an evaluation model for assessing active travel environments and urban design coordination [23]. This model evaluated 12 streets in Zhongnanhu District, Handan City, Hebei Province. The study found that TOPSIS is suitable for examining active travel environments. However, using Euclidean distance encountered challenges in scale, and the relative closeness calculation method within TOPSIS lacked sufficient stability. DEA is a comparative ranking method that evaluates indicators [24]. Cheng employed the APH-DEA method to evaluate optimal locations for bicycle parking in active travel environments in the Haidian, Chaoyang, and Tongzhou districts of Beijing [25], ranking each parking area based on its merits. Nonetheless, the DEA's classification of subjects solely through ranking may result in certain subjects being considered ineligible despite meeting the required criteria due to their lower ranking.

Extenics stands apart from other evaluation methods due to its distinctive characteristics. Firstly, Extenics does not impose a uniform scale, allowing each indicator to possess its independent scale. This flexibility enables the simultaneous evaluation of multiple indicators with varying scales. It also permits adjustments based on varying standards across different regions, thus enabling adaptation to various scenarios. Furthermore, the classification criteria for different grades in the Extenics evaluation remain fixed, eliminating the need for indicator ranking. Instead, indicators that meet specific criteria are assigned to corresponding levels, thereby avoiding potential errors or omissions.

Extenics, pioneered by Professor Wen Cai, employ formalized models to explore the potential expansion possibility of various objects. Furthermore, Extenics facilitates the generation of innovative methods and optimal strategies through evaluation [26]. The application of Extenics has been extensive, including studies on urban road quality evaluation and road development assessments. Ling applied Extenics to conduct a comprehensive evaluation of pavement performance. By employing Extenics evaluation, even objects within the same grade could exhibit discernible differences, formulating maintenance and repair strategies [27]. Cheng applied Extenics to evaluate urban road intersections and compared them with other methods, such as grayscale and fuzzy analyses. Extenics evaluates specific indicators and provides a simultaneous assessment of intersection safety across the entire city, thus offering reliable and objective strategies [28]. In active travel, Chen et al. used the Extenics method to construct an evaluation model for the bicycle travel system. They derived optimization strategies based on the evaluation results, which were subsequently employed to propose adjustments for the bicycle travel system in Taixing City [29]. While the indicators in this study primarily focused on road network planning for bicycle transportation rather than facilities, the applicability of Extenics in the realm of active travel is demonstrated from a macro planning perspective. Moreover, the research focused solely on assessing the existing conditions of the bicycle travel system, and no specific measures or recommendations for improvement were derived from the evaluation outcomes.

In summary, the pandemic has brought greater pressure and safety risks to active travel around hospitals[16–19]. However, current research on active travel lacks attention to hospitals, and the evaluation criteria are relatively broad[20–22], making it difficult to

devise strategies based on evaluation results [29]. Therefore, this study aims to develop an evaluation system for active travel environments around large urban hospitals. Simultaneously, this system should be capable of optimizing the hospital's surrounding travel environment and reducing traffic congestion and risks based on the evaluation results. Moreover, this study utilizes Extenics theory as an evaluation tool, which is more flexible and accurate compared to other methods[27,28]. In contrast to existing research, the novelty of this study lies not only in proposing a new set of evaluation criteria but also in employing Extenics theory to establish a comprehensive logical chain from problem identification to core issue localization and solution generation. This provides valuable insights for policymakers and researchers in related fields.

The subsequent sections of this paper are structured as follows: Section 2 presents an overview of the entire evaluation system and details the process of constructing the Extenics evaluation model. Section 3 applies the evaluation method to a practical case to obtain quantitative data. Then, Section 4 analyzes the evaluation results and provides strategies to assess the feasibility and validity of the evaluation method. Finally, Section 5 outlines the limitations of this study and proposes directions for future research.

2. Method

This section describes the construction of the evaluation system and the details of the Extenics evaluation method.

2.1. Construction of evaluation system

In the previous studies, Teng introduced an assessment index system for facilities to fulfill active travelers' safety, equity, convenience, and psychological comfort requirements [20]. In this section, based on existing research [20–22,29], this study presents a novel set of evaluation indexes specifically tailored for active travel surrounding urban hospitals. These indexes are categorized into five aspects: Safety, Accessibility, Traffic pressure, Convenience, and Comfortableness.

2.1.1. Safety

Pedestrians and cyclists are vulnerable when they come into contact with motor vehicles during active travel [30]. Furthermore, secure hardware facilities can increase participation in active travel [31,32]. This metric evaluates whether the road infrastructure provides enough space for pedestrians and cyclists. Hence, the primary focus of this indicator is to assess whether the sidewalks and bicycle lanes meet national standards [33,34]. Additionally, parking occupancy and other factors are also considered in the evaluation criteria. Indicators and calculation methods are shown in Table 1.

2.1.2. Accessibility

Greater emphasis should be placed on providing adequate care for individuals with limited mobility around hospitals. This indicator assesses the availability of tactile pavements along pedestrian pathways, the presence of ramps adjacent to roads, and the installation of audible signals at intersections [35,36]. The indicators are shown in Table 2.

2.1.3. Traffic pressure

This indicator assesses the traffic volume on the road during peak hours. Additionally, the distribution of different traffic modes is utilized to determine the primary source of traffic on the road during the peak period. Pedestrian density denotes the number of

Table 1
Evaluation index of safety.

Tier 1 Indicator	Tier 2 Indicators	Calculation	Note
Safety	Sidewalk occupied rate [20]	$Y_1 = \frac{L_1^{'}}{L_1}$	$L_1^{'}$ = Sidewalk occupancy length by road facilities, parking facilities, and other elements (m). L_1 = Total length of the sidewalk (m)
	Non-motorized lane occupied rate	$Y_2 = \frac{L_2^{'}}{L_2}$	$L_2^{'}$ = non-motorized lane occupancy length by road facilities, parking facilities, and other elements (m). L_2 = Total length of the non-motorized lane (m)
	Non-motorized lane separation rate [37]	$Y_3 = I_3$, $(I_3 = 1, 0.9, 0.8, 0.7)$	Total separated (90%–100%): $I_3 = 1$; mostly separated (> 50%) $I_3 = 0.9$; few separated (< 50%) $I_3 = 0.8$; no separation $I_3 = 0.7$.
	Sidewalk sub-panel status [37]	$Y_4 = I_4$, $(I_4 = 1, 0.9, 0.8, 0.7)$	Total sub-panelled (90%–100%): $I_4 = 1$; mostly sub-panelled (> 50%): $I_4 = 0.9$; few sub-panelled (< 50%): $I_4 = 0.8$; no sub-panel: $I_4 = 0.7$.
	Non-motorized lane width compliance rate [34]	$Y_5 = \frac{\sum_{i=1}^{n}\left(\frac{l_i}{l_m} \times w_i\right)}{w_r}$	l_i = Corresponding length of the non-motorized lanes in different widths; w_i = the actual width of the non-motorized lane; w_r = the standard width of the non-motorized lane
	Sidewalk width compliance rate	$Y_6 = \frac{\sum_{j=1}^{n}\left(\frac{l_j}{l_m} \times w_j\right)}{w_r}$	l_j = Corresponding length of the sidewalk in different widths; w_j = the actual width of the sidewalk; w_j = the standard width of the sidewalk

Table 2
Evaluation index of accessibility.

Tier 1 Indicator	Tier 2 Indicators	Calculation	Note
Accessibility	Tactile paving coverage	$Y_7 = \frac{L_7^{'}}{L_7}$	$L_7^{'}$ = Length of the Tactile paving (m); L_7 = Total length of the sidewalk (m)
	Curbs with ramps coverage	$Y_8 = \frac{L_8^{'}}{L_8}$	$L_8^{'}$ = Number of curb junctions with ramps; L_8 = Total number of road junctions
	Acoustic signalized intersections coverage [20]	$Y_9 = \frac{L_9^{'}}{L_9}$	$L_9^{'}$ = Number of acoustic signalized intersections; L_9 = Total number of road junctions

individuals passing through within a given time frame, and if it surpasses a specific threshold, it is regarded as congestion. The level of mixed motor/non-motor traffic indicates the proportion of motor vehicles to non-motor vehicles passing through within the same time frame, and a higher percentage signifies a greater number of motor vehicles—similarly, the non-motor/pedestrian traffic mix. The indicators are shown in Table 3.

2.1.4. Convenience

The road must offer convenience for individuals accessing the hospital and residing in the surrounding neighborhood. This indicator evaluates the extent of interchange facilities and crossing facilities available. Also, the road grade may affect its reachability [37]. And the indicators are shown in Table 4.

2.1.5. Comfortableness

A pleasant travel environment ensures a comfortable experience for pedestrians and cyclists. Moreover, well-developed urban green infrastructure plays a crucial role in enhancing the resilience of cities and their inhabitants in the face of a pandemic [38]. Hence, this indicator assesses various environmental factors that have the potential to influence individuals engaging in active travel. And the indicators are shown in Table 5.

2.2. Determination of the weights of the indicators

After establishing the evaluation system, it is necessary to allocate weights to each indicator, with a greater weight assigned to indicators of greater significance. The general approach employed for this purpose is the Analytic Hierarchy Process (AHP), which determines weights by assessing the relative sizes of indicator numbers, often requiring the input of experts [39]. After distributing questionnaires, 30 valid responses were obtained from experts, including designers and scholars specializing in architectural design, urban planning, and environmental design, as well as doctors and staff working in major hospitals. And the results were obtained as in Table 6.

2.2. Establishment of the Extenics evaluation model

2.2.1. Establishment of the matter-element model

Matter-element is a logical cell within Extenics that conveys both the characteristics of an object and the corresponding character values. It consists of three components: the object $\boldsymbol{P}$, the characteristic $\boldsymbol{c}$, and the value $\boldsymbol{v}$. And it can be noted as:

$$M = (P, c, v) \tag{1}$$

If $\boldsymbol{M}$ contains multiple characteristics: $c_1, c_2, \ldots c_n$. And the corresponding quantity value are $v_1, v_2, \ldots, v_n$. Then the matter-element model can be indicated as:

Table 3
Evaluation Index of Traffic pressure.

Tier 1 Indicator	Tier 2 Indicators	Calculation	Note
Traffic pressure	Peak crowd density	$Y_{10} = \frac{N}{t \times s}$	N = Total number of people passing through the observation area per unit of time; t = unit time s = Observation area size (m^2)
	Peak non-motorized vehicles/Motor vehicles mix	$Y_{11} = \frac{P_{11}}{P_{11} + Q_{11}}$	P_{11} = Non-motorized traffic volume during peak hours (V/h); Q_{11} = Motorized traffic volume during peak hours (V/h)
	Peak pedestrian/non-motorized vehicles mix [34]	$Y_{12} = \frac{P_{12}}{P_{12} + Q_{12}}$	P_{12} = pedestrian volume during peak hours (P/h); Q_{12} = Non-motorized traffic volume during peak hours (V/h)

Table 4
Evaluation index of convenience.

Tier 1 Indicator	Tier 2 Indicators	Calculation	Note
Convenience	Interchange site coverage	$Y_{13} = \frac{R_{13}}{L_{13}}$	R_{13} = The length of the road covered within a radius of 500 m, with the interchange node as the center.; L_{13} = Total length of the street
	Street crossing facility coverage	$Y_{14} = \frac{R_{14}}{L_{14}}$	R_{14} = The length of the road covered within a radius of 200 m, with the crossing facility as the center.; L_{14} = Total length of the street
	Road grade [37]	$Y_{15} = I_{15}$, $(I_{15} = 0.8, 0.9)$	Urban expressways and arterial roads: $I_{15} = 0.8$ Secondary arterial roads or local roads: $I_{15} = 0.9$

Table 5
Evaluation index of comfortableness.

Tier 1 Indicator	Tier 2 Indicators	Calculation	Note
Comfortableness	Interface permeability [22]	$Y_{16} = \frac{D_1 \times 1.25 + D_2 \times 1.0 + D_3 \times 0.75 + D_4 \times 0}{L_{16}}$	D_1 = Length of the open façade D_2 = Length of the transparent façade D_3 = Length of the transparent window D_4 = Length of the opaque solid wall L_{16} = Total length of the underlying interface
	Road flatness	$Y_{17} = I_{17}$, $(I_{17} = 1, 0.9, 0.8)$	Flattened: $I_{17} = 1$ The road surface exhibits minor unevenness, but it does not impede usability: $I_{17} = 0.9$ The road is rough and uneven: $I_{17} = 0.8$
	Road cleanliness [37]	$Y_{18} = I_{18}$, $(I_{18} = 1, 0.9, 0.8)$	Clean: $I_{18} = 1$ There is some litter present on the road: $I_{18} = 0.9$ The road is littered with a significant amount of trash, making it difficult to clean and resulting in stains and unpleasant odors.: $I_{18} = 0.8$
	Resting seat setting coverage [20]	$Y_{19} = 0.5\frac{E'}{E} + 0.5g, g < 1$	E' = Number of bus stops with seats; E = Number of bus stops; g = Average number of seats within 200 m in the study area
	Street tree pond coverage	$Y_{20} = \frac{w'}{W}$	w' = Width of green belt with trees planted W = Road red line width

Table 6
Evaluation indicators weights of active travel environment around hospitals.

Tier 1 Indicators	Weights	Tier 2 Indicators	Weights
Safety (B_1)	0.40272	Sidewalk occupied rate (C_1)	0.09498
		Non-motorized lane occupied rate (C_2)	0.0566
		Non-motorized lane separation rate (C_3)	0.06616
		Sidewalk sub-panel status (C_4)	0.05468
		Non-motorized lane width compliance rate (C_5)	0.06902
		Sidewalk width compliance rate (C_6)	0.06128
Accessibility (B_2)	0.19288	Tactile paving coverage (C_7)	0.08018
		Curbs with ramps coverage (C_8)	0.05808
		Acoustic signalized intersections coverage (C_9)	0.05462
Traffic pressure (B_3)	0.25592	Peak crowd density (C_{10})	0.13298
		Peak non-motorized vehicles/Motor vehicles mix (C_{11})	0.06538
		Peak pedestrian/non-motorized vehicles mix (C_{12})	0.05756
Convenience (B_4)	0.08052	Interchange site coverage (C_{13})	0.03464
		Street crossing facility coverage (C_{14})	0.03316
		Road grade (C_{15})	0.01272
Comfortableness (B_5)	0.06796	Interface permeability (C_{16})	0.01302
		Road flatness (C_{17})	0.0207
		Road cleanliness (C_{18})	0.01248
		Resting seat setting coverage (C_{19})	0.0107
		Street tree pond coverage (C_{20})	0.01106

$$M = \begin{bmatrix} P, & c_1, & v_1 \\ & c_2, & v_2 \\ & \cdots & \cdots \\ & c_n, & v_n \end{bmatrix} \tag{2}$$

2.2.2. Determination of the classical domain, nodal domain, and the matter-element

The classical domain matter-element, denoted as $\boldsymbol{M_j}$, represents the range of values (a_j, b_j) of an indicator at a specific grade. In evaluations, a single indicator has multiple ranges of values across different classical domains. Distinct ranges represent different levels of superiority or inferiority. If a certain grade is $\boldsymbol{P_j}$, the indicator is expressed as c_i, and the range of value is v_j. The classical domain matter-element $\boldsymbol{M_j}$ can be expressed as:

$$M_j = (P_j, c_j, v_{ji}) = \begin{bmatrix} P_j, & c_1, & v_{j1} \\ & c_2, & v_{j2} \\ & \cdots & \cdots \\ & c_n, & v_{jn} \end{bmatrix} = \begin{bmatrix} P_j, & c_1, & \langle a_{j1}, & b_{j1} \rangle \\ & c_2, & \langle a_{j2}, & b_{j2} \rangle \\ & \cdots & & \cdots \\ & c_n, & \langle a_{jn}, & b_{jn} \rangle \end{bmatrix} \tag{3}$$

The nodal domain is the overall range of values for an indicator. The nodal domain matter-element $\boldsymbol{P_p}$ contains three parts. The nodal domain $\boldsymbol{P}$, indicators c_i and values v_{pi}. and it can be expressed as:

$$M_p = (P, c_{pi}, v_{pi}) = \begin{bmatrix} P, & c_1, & v_1 \\ & c_2, & v_2 \\ & \cdots & \cdots \\ & c_n, & v_n \end{bmatrix} \tag{4}$$

Before evaluating, it is necessary to transform each street into a matter-element model. Once the transformation is completed, the evaluation can be carried out using the methodology of Extenics. Based on equation (1) and equation (2), consider road $\boldsymbol{P}$ as the object, representing the active travel road matter-element $\boldsymbol{M_0}$, encompassing indicators c_0 and corresponding data v_0 obtained from field surveys. The model can be established as follows:

$$M_0 = (P, c_i, v_i) = \begin{bmatrix} P, & c_1, & v_1 \\ & c_2, & v_2 \\ & \cdots & \cdots \\ & c_n, & v_n \end{bmatrix} \tag{5}$$

2.2.3. Determining the association between the values and classical domains

The Extenics evaluation method considers the quantitative values within a matter-element as points on an axis. It determines the degree of conformity between the value and a specified range. After obtaining the quantitative value (v_i) of the road matter-element ($\boldsymbol{M_0}$), it is necessary to calculate the association degree $\boldsymbol{K_i(v_i)}$ between this data and each different value range (a, b) corresponding to its classical domain (vji). The specific calculation can be expressed as follows

$$K_j(v_i) = \begin{cases} \dfrac{\rho(v_i, v_{ji})}{\rho(v_i, v_{pi}) - \rho(v_i, v_{ji})}, (v_i \notin v_{ji}) \\ -\dfrac{\rho(v_i, v_{pi})}{|v_{ji}|}, (v_i \in v_{ji}) \end{cases} \tag{6}$$

Where:

$$\rho(v_i, v_{ji}) = \left| v_i - \frac{a_{ji} + b_{ji}}{2} \right| - \frac{b_{ji} - a_{ji}}{2}$$

$$\rho(v_i, v_{pi}) = \left| v_i - \frac{a_{pi} + b_{pi}}{2} \right| - \frac{b_{pi} - a_{pi}}{2}$$

$$|v_{ji}| = |a_{ji} - b_{ji}|$$

2.2.4. Determination of association degree and evaluation

Extenics examines the association value $\boldsymbol{K_j(P)}$ between a matter-element and each different level (excellent, good, moderate, poor, very poor) to derive the comprehensive evaluation result $\boldsymbol{K_{j0}}$.

The association value $\boldsymbol{K_j(P)}$ for the indicator i concerning level j (i.e., classic domain) is obtained by multiplying the $\boldsymbol{K_j(v_i)}$ value by its corresponding weight, resulting in $\lambda_i K_j(v_i)$. Subsequently, the $\lambda_i K_j(v_i)$ values for all metrics located within the level j are summed together, yielding the association value $\boldsymbol{K_j(P)}$:

$$K_j(P) = \sum_{i=1}^{n} \lambda_i K_j(v_i) \tag{7}$$

Subsequently, the obtained $K_j(P)$ values are compared to determine the highest value. The level corresponding to the maximum $K_j(P)$ value represents the comprehensive evaluation result K_{j0} for the road:

$$K_{j0} = max\ K_j(P), (j = 1, 2, ..., m) \tag{8}$$

(1) If K_{j0} <-1, it indicates that the indicator does not meet the criteria for the grade.
(2) If $-1 \leq K_{j0} < 0$, it also means that the indicator does not meet the demand of the grade, but it is possible to be converted to meet the demand.
(3) If $0 \leq K_{j0} < 1$, it indicates that the indicator meets the requirements of the grade.

3. Validation

This study focuses on Xiangya Hospital and its surrounding area in the Kaifu District, the center of Changsha. This region comprises three national-certified top-tier hospitals, each differing in size but maintaining a high standard of medical services, and these hospitals are highly renowned. The research area was defined based on the location of interchange nodes, as depicted in Fig. 1. It is delineated by Xiangya Road, Furong Middle Road, Yingpan Road, and Huangxing North Road, encompassing internal streets such as Xiangchun Road, Cai E North Road, and other internal alleyways.

After considering the distance and transfer nodes, this study divides the selected area into two parts for calculations and evaluations (as shown in Fig. 2).

3.1. Regional status analysis

The population residing in Kaifu District, Changsha, exceeds 850,000 individuals [40], and electric bicycles serve as a prevalent mode of transportation for Changsha's residents. By 2020, the number of electric bicycles had surpassed one million [41], contributing to significant pedestrian and non-motorized traffic during peak hours.

The area comprises six arterial roads: Xiangya Road, Furong Middle Road, Xiangchun Road, Cai E North Road, Yingpan Road, and Huangxing North Road. During peak hours, the traffic volume on these roads tends to concentrate towards the hospitals (as Fig. 3 shows). During the field research, it was found that these roads generally have relatively complete infrastructure and rarely experience missing sidewalks or accessibility facilities. However, there are issues such as road occupation due to construction and parking (as Fig. 4 shows), and some roads neglect the provision of non-motorized lanes (as Fig. 5 shows). The ground floor interface of the buildings primarily includes hospitals, shops, restaurants, pharmacies, and supermarkets, and it is relatively compact.

On the other hand, the internal alleys are closely connected to the residents' daily lives in the area. In Sector M, the main focus is residential neighborhoods, while Sector N includes a morning market, vegetable market, and, notably, two adjacent kindergartens and elementary schools. Many parents commute to drop off their children during rush hour, resulting in a relatively dense presence of pedestrians and non-motorized vehicles. However, during the research, it was discovered that these alleys are generally narrow. To accommodate motor vehicles, there are instances where pedestrian sidewalks are not separated, creating a situation where various modes of transportation intersect during peak hours and increasing safety hazards (as Fig. 6 shows). Moreover, the lack of sidewalks

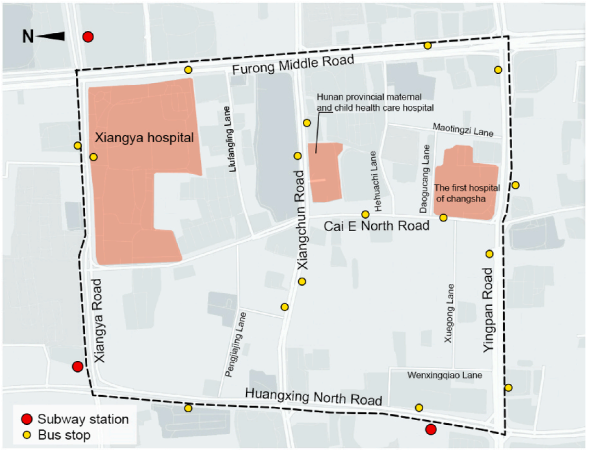

Fig. 1. A map of the research area.

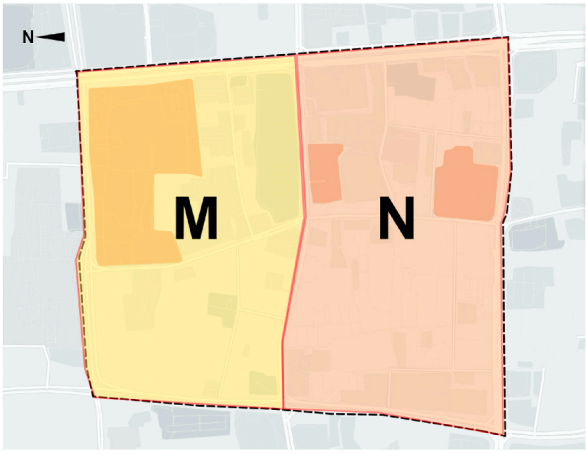

Fig. 2. A demonstration of sections.

Fig. 3. Concentrated traffic volume.

Fig. 4. Construction and parking occupation.

also prevents the installation of other facilities, such as tactile paving and resting seats, creating obstacles and inconveniences for the residents' mobility (as Fig. 7 shows).

3.2. Data of indicators

This study primarily employed on-site surveys to gather data on the roads. Measurements were taken using tools to record pedestrian sidewalk width, non-motorized lane width, length of facilities occupancy, length of different road surface interfaces, and width of roadside tree green spaces et al. During peak hours, fixed-point observations were conducted on each street to record the volume of vehicles, pedestrians, and non-motorized vehicles passing through. Additionally, mapping software was utilized to obtain the data for certain aspects that were difficult to measure on-site (such as coverage of transfer stations and pedestrian crossing

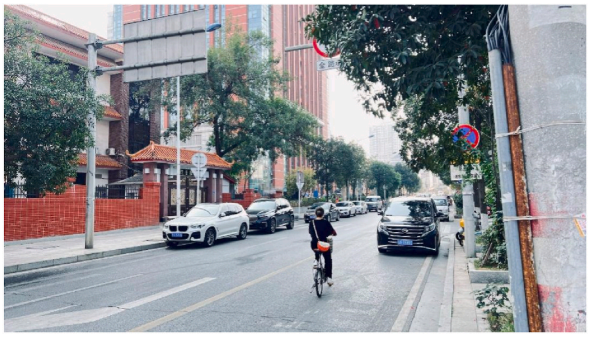

Fig. 5. non-motorized lanes missing.

Fig. 6. Narrow alley and mixed traffic.

Fig. 7. Obstacles for the residents.

facilities). Through a combination of field surveys and calculations, data for each street was obtained. Furong Middle Road is shown in Table 7 below as an example (see supporting materials for other roads).

3.3. Association calculation and grade rating

3.3.1. Determine the classical and nodal domains of the indicators to be evaluated

According to equation (3) and equation (4), the evaluation grades are categorized into five levels: "Excellent, Good, Moderate, Poor, Very poor," ranked from best to worst, and are represented as P_1, P_2, P_3, P_4, and P_5, respectively. The value ranges for the classical and nodal domains are determined based on expert opinions and relevant criteria. The classical domains R_1, R_2, R_3, R_4, R_5, and the nodal domain P_p are defined as follows:

Table 7
Furong Middle Road indicators data.

Street	Indicator	Value	Street	Indicator	Value
West side of Furong Middle Road	C_1	0.189	East side of Furong Middle Road	C_1	0.511
	C_2	0		C_2	0
	C_3	0.8		C_3	0.8
	C_4	1		C_4	1
	C_5	0.746		C_5	0.48
	C_6	1		C_6	1.5
	C_7	0.687		C_7	0.838
	C_8	1		C_8	1
	C_9	0		C_9	0
	C_{10}	8.3		C_{10}	2.01
	C_{11}	0.242		C_{11}	0.237
	C_{12}	0.676		C_{12}	0.517
	C_{13}	1		C_{13}	1
	C_{14}	1		C_{14}	1
	C_{15}	0.8		C_{15}	0.8
	C_{16}	0.497		C_{16}	0.836
	C_{17}	1		C_{17}	1
	C_{18}	1		C_{18}	1
	C_{19}	0.788		C_{19}	0.788
	C_{20}	0.385		C_{20}	0.368

$$R_1 = \begin{bmatrix} P_1 & c_1 & (0,0.2) \\ & c_2 & (0,0.2) \\ & c_3 & (0.95,1) \\ & c_4 & (0.95,1) \\ & c_5 & (1,1.5) \\ & c_6 & (1,1.5) \\ & c_7 & (0.8,1) \\ & c_8 & (0.8,1) \\ & c_9 & (0.8,1) \\ & c_{10} & (0,1.5) \\ & c_{11} & (0,0.3) \\ & c_{12} & (0,0.3) \\ & c_{13} & (0.8,1) \\ & c_{14} & (0.8,1) \\ & c_{15} & (0.95,1) \\ & c_{16} & (0.8,1) \\ & c_{17} & (0.95,1) \\ & c_{18} & (0.95,1) \\ & c_{19} & (0.8,1) \\ & c_{20} & (0.35,0.5) \end{bmatrix} \quad R_2 = \begin{bmatrix} P_2 & c_1 & (0.2,0.4) \\ & c_2 & (0.2,0.4) \\ & c_3 & (0.85,0.95) \\ & c_4 & (0.85,0.95) \\ & c_5 & (0.75,1) \\ & c_6 & (0.75,1) \\ & c_7 & (0.7,0.8) \\ & c_8 & (0.6,0.8) \\ & c_9 & (0.6,0.8) \\ & c_{10} & (1.5,3) \\ & c_{11} & (0.3,0.5) \\ & c_{12} & (0.3,0.5) \\ & c_{13} & (0.6,0.8) \\ & c_{14} & (0.6,0.8) \\ & c_{15} & (0.85,0.95) \\ & c_{16} & (0.6,0.8) \\ & c_{17} & (0.85,0.95) \\ & c_{18} & (0.85,0.95) \\ & c_{19} & (0.6,0.8) \\ & c_{20} & (0.3,0.35) \end{bmatrix} \quad R_3 = \begin{bmatrix} P_3 & c_1 & (0.4,0.6) \\ & c_2 & (0.4,0.6) \\ & c_3 & (0.75,0.85) \\ & c_4 & (0.75,0.85) \\ & c_5 & (0.5,0.75) \\ & c_6 & (0.5,0.75) \\ & c_7 & (0.6,0.7) \\ & c_8 & (0.4,0.6) \\ & c_9 & (0.4,0.6) \\ & c_{10} & (3,4.5) \\ & c_{11} & (0.5,0.6) \\ & c_{12} & (0.5,0.6) \\ & c_{13} & (0.4,0.6) \\ & c_{14} & (0.4,0.6) \\ & c_{15} & (0.75,0.85) \\ & c_{16} & (0.4,0.6) \\ & c_{17} & (0.75,0.85) \\ & c_{18} & (0.75,0.85) \\ & c_{19} & (0.4,0.6) \\ & c_{20} & (0.25,0.3) \end{bmatrix}$$

$$R_4 = \begin{bmatrix} P_4 & c_1 & (0.6,0.8) \\ & c_2 & (0.6,0.8) \\ & c_3 & (0.65,0.75) \\ & c_4 & (0.65,0.75) \\ & c_5 & (0.25,0.5) \\ & c_6 & (0.25,0.5) \\ & c_7 & (0.5,0.6) \\ & c_8 & (0.2,0.4) \\ & c_9 & (0.2,0.4) \\ & c_{10} & (4.5,6) \\ & c_{11} & (0.6.0.8) \\ & c_{12} & (0.6.0.8) \\ & c_{13} & (0.2,0.4) \\ & c_{14} & (0.2,0.4) \\ & c_{15} & (0.65,0.75) \\ & c_{16} & (0.2,0.4) \\ & c_{17} & (0.65,0.75) \\ & c_{18} & (0.65,0.75) \\ & c_{19} & (0.2,0.4) \\ & c_{20} & (0.2,0.25) \end{bmatrix} \quad R_5 = \begin{bmatrix} P_5 & c_1 & (0.8,1) \\ & c_2 & (0.8,1) \\ & c_3 & (0,0.65) \\ & c_4 & (0,0.65) \\ & c_5 & (0,0.25) \\ & c_6 & (0,0.25) \\ & c_7 & (0,0.5) \\ & c_8 & (0,0.2) \\ & c_9 & (0,0.2) \\ & c_{10} & (6,10) \\ & c_{11} & (0.8,1) \\ & c_{12} & (0.8,1) \\ & c_{13} & (0,0.2) \\ & c_{14} & (0,0.2) \\ & c_{15} & (0,0.65) \\ & c_{16} & (0,0.2) \\ & c_{17} & (0,0.65) \\ & c_{18} & (0,0.65) \\ & c_{19} & (0,0.2) \\ & c_{20} & (0,0.2) \end{bmatrix} \quad P_p = \begin{bmatrix} P_p & c_1 & (0,1) \\ & c_2 & (0,1) \\ & c_3 & (0,1) \\ & c_4 & (0,1) \\ & c_5 & (0,1.5) \\ & c_6 & (0,1.5) \\ & c_7 & (0,1) \\ & c_8 & (0,1) \\ & c_9 & (0,1) \\ & c_{10} & (0,10) \\ & c_{11} & (0,1) \\ & c_{12} & (0,1) \\ & c_{13} & (0,1) \\ & c_{14} & (0,1) \\ & c_{15} & (0,1) \\ & c_{16} & (0,1) \\ & c_{17} & (0,1) \\ & c_{18} & (0,1) \\ & c_{19} & (0,1) \\ & c_{20} & (0,0.5) \end{bmatrix}$$

3.3.2. Establishment of a matrix of matter-elements

Before building the matrix, each street is transformed into an Extenics matter-elements as shown in Table 8 and Table 9.

According to Equation (5), the matter-elements matrixes can be established (M_3, for example. Other roads are omitted):

$$M_3 = \begin{bmatrix} P_3 & c_{31} & 0.189 \\ & c_{32} & 0 \\ & c_{33} & 0.8 \\ & c_{34} & 1 \\ & c_{35} & 0.746 \\ & c_{36} & 1 \\ & c_{37} & 0.687 \\ & c_{38} & 1 \\ & c_{39} & 0 \\ & c_{310} & 8.3 \\ & c_{311} & 0.242 \\ & c_{312} & 0.676 \\ & c_{313} & 1 \\ & c_{314} & 1 \\ & c_{315} & 0.8 \\ & c_{316} & 0.497 \\ & c_{317} & 0.8 \\ & c_{318} & 1 \\ & c_{319} & 0.788 \\ & c_{320} & 0.385 \end{bmatrix}$$

3.3.3. Determination of the association degree of each road regarding different grades

According to equation (6), each road's nodal and classical domain values can be derived, as Table 10 shows. (M_3, for example. See supporting materials for other roads).

According to equation (7), the obtained classical domain values for each indicator are multiplied by their corresponding weights, resulting in the following outcome (as Table s11 and 12 indicate).

According to equation (7), The comprehensive association value can be determined by summing up the association values of each indicator within the same grade, thereby allowing the classification of the road into its corresponding level (as shown in Table s13 and 14).

According to Table 13, Table 14 and Equation (8), the comprehensive evaluation of the active travel environment around Xiangya Hospital can be derived as shown in Fig. 8.

4. Discussion

It can be observed from Fig. 8 that the active travel environment around Xiangya Hospital is generally in a mediocre state, according to the overall evaluation. Out of the 34 road samples, only seven roads are rated as "Good" or above, while eight are rated as "Poor" or below. The remaining roads fall into the "Moderate" category, accounting for approximately 44% of the total roads. There is much room to improve active travel in the area.

4.1. Identification of the primary issues and target roads

Following the comprehensive evaluation analysis mentioned above, the overall performance of the active transportation spaces in the region was obtained. The next step involves examining the evaluation level of every tire one indicator on each road, identifying the existing issues within the study area, and pinpointing the roads with more apparent problems among the various indicators. This process aims to identify optimization objectives and develop targeted strategies for improvement.

Fig. 9 shows that the roads in the area perform poorly regarding the "Safety" indicator. Only ten roads fall under the "Good" or higher category, while 14 are categorized as "Poor" or lower. Regarding rating patterns, the areas with lower safety ratings are predominantly concentrated in the internal alleys, which aligns with the issues identified during the research.

Table 8
Streets and corresponding matter-elements in Section M.

Street	Matter-element	Street	Matter-element
The south side of Xiangya Road	M_1	The east side of Cai E North Road	M_8
The north side of Xiangya Road	M_2	The south side of Pengjiajing Lane	M_9
The west side of Furong Middle Road	M_3	The north side of Pengjiajing Lane	M_{10}
The east side of Furong Middle Road	M_4	The west side of Pengjiajing Lane	M_{11}
the west side of Huangxing North Road	M_5	The east side of Pengjiajing Lane	M_{12}
The east side of Huangxing North Road	M_6	The south side of Liufangling Lane	M_{13}
The west side of Cai E North Road	M_7	The north side of Liufangling Lane	M_{14}

Table 9
Streets and corresponding matter-elements in Section N.

Street	Matter-element	Street	Matter-element
The south side of Xiangchun Road	N_1	The west side of Wenxingqiao Lane	N_{11}
The north side of Xiangchun Road	N_2	The east side of Wenxingqiao Lane	N_{12}
The south side of Yingpan Road	N_3	The south side of Xuegong Lane	N_{13}
The north side of Yingpan Road	N_4	The north side of Xuegong Lane	N_{14}
The west side of Huangxing North Road	N_5	The south side of Hehuachi Lane	N_{15}
The east side of Huangxing North Road	N_6	The north side of Hehuachi Lane	N_{16}
The west side of Furong Middle Road	N_7	The south side of Daogucang Lane	N_{17}
The east side of Furong Middle Road	N_8	The north side of Daogucang Lane	N_{18}
The west side of Cai E North Road	N_9	The west side of Maotingzi Lane	N_{19}
The east side of Cai E North Road	N_{10}	The east side of Maotingzi Lane	N_{20}

Table 10
M_3's classical and nodal domain values.

Indicator	Nodal domain value	Classical domain value				
		Excellent	Good	Moderate	Poor	Very poor
C_1	−0.189	0.945	−0.055	−0.528	−0.685	−0.764
C_2	0	0	−1	−1	−1	−1
C_3	−0.2	−0.429	−0.2	2	−0.2	−0.429
C_4	0	0	−1	−1	−1	−1
C_5	−0.746	−0.254	−0.005	2.984	−0.248	−0.339
C_6	−0.5	1	0	−0.2	−0.5	−0.6
C_7	−0.313	−0.265	−0.040	3.13	−0.218	−0.374
C_8	0	0	−1	−1	−1	−1
C_9	0	−1	−1	−1	−1	0
C_{10}	−1.7	−0.8	−0.757	−0.691	−0.575	0.425
C_{11}	−0.058	0.193	−0.5	−0.816	−0.861	−0.906
C_{12}	−0.324	−0.537	−0.352	−0.19	1.62	−0.277
C_{13}	0	0	−1	−1	−1	−1
C_{14}	0	0	−1	−1	−1	−1
C_{15}	−0.2	−0.429	0.02	2	−0.02	−0.429
C_{16}	−0.497	−0.379	−0.172	2.485	−0.163	−0.383
C_{17}	0	0	−1	−1	−1	−1
C_{18}	0	0	−1	−1	−1	−1
C_{19}	−0.212	−0.054	1.06	−0.47	−0.647	−0.735
C_{20}	−0.115	0.767	−0.233	−0.425	−0.54	−0.617

Table 11
M_3 tire 1 indicator association K value.

Indicator	Association K value				
	Excellent	Good	Moderate	Poor	Very poor
B_1	0.10512238	−0.130081	0.16459024	−0.23733026	−0.27239314
B_2	−0.0758677	−0.1159072	0.1382634	−0.13017924	−0.08806732
B_3	−0.12467538	−0.15361698	−0.04236	−0.03950848	−0.0186619
B_4	−0.00545688	−0.0675456	−0.04236	−0.0680544	−0.07325688
B_5	0.00297064	−0.02665442	−0.0105548	−0.04819756	−0.05285518

Fig. 10 indicates that on arterial roads, the provision of accessibility facilities is relatively complete and reliable, resulting in better ratings. However, significant neglect in installing accessibility-related facilities within the internal alleys leads to serious deficiencies.

Based on Fig. 11, it can be observed that the roads on the side adjacent to the hospital received lower evaluation ratings compared to the opposite side. This indicates that the hospital exerts a stronger influence on the surrounding traffic during peak hours, resulting in higher traffic volume and congestion than the opposite side. Furthermore, traffic pressure during peak hours can be observed in the eastern half of the internal alleys in Sector N. This area coincides with the vicinity of the observed kindergartens and elementary schools during the research, where significant traffic flow is experienced during the morning rush hour. The evaluation confirms the findings observed during the research.

Thanks to the relatively dense interchange and pedestrian crossing facilities, the accessibility rating in the area is generally high, facilitating convenient access for pedestrians and cyclists from transportation nodes to any location within the area, as Fig. 12 shows.

As Fig. 13 indicates, In terms of comfort, most streets receive ratings categorized as "good" or above, indicating that the environment, landscaping, and ground-level interface of the roads within the area are generally favorable. Relatively lower ratings are mainly observed in the internal alleys.

Table 12
M_3 tire 2 indicator association K value.

Indicator	Association K value				
	Excellent	Good	Moderate	Poor	Very poor
C_1	0.0897561	−0.0052239	−0.05014944	−0.0650613	−0.07256472
C_2	0	−0.0566	−0.0566	−0.0566	−0.0566
C_3	−0.02838264	−0.013232	0.13232	−0.013232	−0.02838264
C_4	0	−0.05468	−0.05468	−0.05468	−0.05468
C_5	−0.01753108	−0.0003451	0.20595568	−0.01711696	−0.02339778
C_6	0.06128	0	−0.012256	−0.03064	−0.036768
C_7	−0.0212477	−0.0032072	0.2509634	−0.01747924	−0.02998732
C_8	0	−0.05808	−0.05808	−0.05808	−0.05808
C_9	−0.05462	−0.05462	−0.05462	−0.05462	0
C_{10}	−0.106384	−0.10066586	−0.09188918	−0.0764635	0.0565165
C_{11}	0.01261834	−0.03269	−0.05335008	−0.05629218	−0.05923428
C_{12}	−0.03090972	−0.02026112	−0.0109364	0.0932472	−0.01594412
C_{13}	0	−0.03464	−0.03464	−0.03464	−0.03464
C_{14}	0	−0.03316	−0.03316	−0.03316	−0.03316
C_{15}	−0.00545688	0.0002544	0.02544	−0.0002544	−0.00545688
C_{16}	−0.00493458	−0.00223944	0.0323547	−0.00212226	−0.00498666
C_{17}	0	−0.0207	−0.0207	−0.0207	−0.0207
C_{18}	0	−0.01248	−0.01248	−0.01248	−0.01248
C_{19}	−0.0005778	0.011342	−0.005029	−0.0069229	−0.0078645
C_{20}	0.00848302	−0.00257698	−0.0047005	−0.0059724	−0.00682402

Table 13
M_1 to M_{14}'s indicator association value.

Street	Association value (K)				
	Excellent	Good	Moderate	Poor	Very poor
M_1	−0.25398654	−0.17505802	0.38485748	0.2695731	−0.40185024
M_2	−0.0990497	0.22234064	−0.51187162	−0.45596336	−0.041778573
M_3	−0.09790694	−0.4938052	0.09376318	−0.52326994	−0.50523442
M_4	−0.0501097	−0.31512738	−0.02530718	−0.60156528	−0.65736912
M_5	0.11942116	−0.35070028	−0.23284934	−0.35889272	−0.70781484
M_6	0.1108701	−0.1969079	−0.06302924	−0.40283566	−0.695322
M_7	−0.4107918	0.08863518	−0.29674924	−0.31503176	−0.64637106
M_8	−0.21685462	−0.10992568	0.03038692	−0.26281028	−0.60466092
M_9	−0.31554528	−0.51555636	−0.17196108	−0.1746031	−0.3532527
M_{10}	−0.31194774	−0.45751002	−0.5225662	−0.19221932	−0.39991652
M_{11}	−0.42869594	−0.58196304	−0.2156315	−0.0581158	−0.38359272
M_{12}	−0.34186186	−0.57588736	−0.54321326	−0.44318804	−0.4570417
M_{13}	−0.4256653	−0.3177992	0.25644952	−0.38377284	−0.42089628
M_{14}	−0.37932914	−0.55374424	0.17794798	−0.26815432	−0.4177994

4.2. Generation of optimization strategies

After identifying the main issues in the study area and target roads, the generation of optimization strategies is guided by analyzing and comparing the evaluation levels of tire two indicators on each road. This analysis allows for a clear identification of the weaknesses in the target roads, facilitating the development of optimization strategies.

Among all road samples, the roads adjacent to hospitals include M_1 and M_2, located at the entrance of the inpatient department of Xiangya Hospital; M_3 and M_4, situated near the outpatient department of Xiangya Hospital; M_9 and M_{10} at the side entrance; N_1 and N_2 found near the outpatient department of Hunan Provincial Maternal and Child Health Care Hospital, N_3 and N_4 close to the outpatient department of Changsha First Hospital, N_9 and N_{10}, which connect these two hospitals.

Firstly, by examining the evaluation results of the "Traffic pressure (B_3)" indicator, it can be determined whether there are issues with the traffic conditions around the hospital during peak hours. Meanwhile, If the road fails to provide a safe and independent environment for pedestrians and cyclists in terms of infrastructure, it is highly likely to lead to traffic accidents. Therefore, it is necessary to simultaneously examine the performance of these roads in terms of the "Safety(B_1)" indicator.

A "Poor" or below road score on the B_3 indicator shows traffic congestion during peak hours. If the road also fails to meet the "Good" criteria on the B_1 indicator, it suggests that the road's safety may be compromised under significant traffic pressure during peak hours. Roads that meet these criteria need to be identified for diversion and isolation measures by analyzing secondary indicators. And these roads are M_1, M_3, and N_1.

M_1 exhibits a "Poor" rating in Peak crowd density (C_{10}), an "Excellent" rating in Peak non-motorized vehicles/Motor vehicles mix (C_{11}), and a "Poor" rating in Peak pedestrian/non-motorized vehicles mix (C_{12}). This indicates that the road experiences a high volume

Table 14
N_1 to N_{20}'s indicator association value.

Street	Association value (K)				
	Excellent	Good	Moderate	Poor	Very poor
N_1	−0.24848252	−0.11575644	0.11354432	0.20554068	−0.45869946
N_2	0.11111006	−0.38545758	0.18607564	−0.1705497	−0.4760777
N_3	−0.12174456	−0.3419058	0.16914826	−0.54189558	−0.52747684
N_4	−0.19639918	0.07209756	−0.59430844	−0.67165968	−0.46996
N_5	0.07943848	0.10267468	−0.48053902	−0.58649708	−0.70085334
N_6	−0.052514	0.40809742	−0.45556878	−0.58335394	−0.63861568
N_7	−0.0262178	0.14596204	−0.33809204	−0.65344504	−0.67156902
N_8	−0.07664154	−0.0846638	−0.40889818	−0.70343904	−0.70960776
N_9	−0.1865003	−0.60563922	−0.4765646	−0.3751296	−0.40698356
N_{10}	−0.28783234	−0.7016794	−0.55945464	−0.51868124	−0.38510382
N_{11}	−0.40707542	−0.57993566	−0.07702116	−0.48458592	−0.3242001
N_{12}	−0.53815116	−0.65707478	−0.11103232	−0.50586372	−0.25298494
N_{13}	−0.9332513	−0.5769689	0.1421789	−0.5491198	−0.3172308
N_{14}	−0.4633754	−0.6228173	0.1697468	−0.5290879	−0.3071703
N_{15}	−0.475271	−0.5380153	−0.69705	−0.5799694	−0.142915
N_{16}	−0.4580989	−0.7558443	−0.758428	−0.6218052	−0.1727285
N_{17}	−0.48227544	−0.61146978	−0.39984652	−0.73020982	−0.31464834
N_{18}	−0.48448884	−0.61442532	−0.40427332	−0.73906342	−0.32350194
N_{19}	−0.5774767	−0.81599838	−0.76655018	−0.65793526	−0.10788286
N_{20}	−0.57331026	−0.79099948	−0.7565643	−0.65706726	−0.12317706

Fig. 8. The comprehensive evaluation results.

of pedestrians during peak hours and frequently interacts with non-motorized vehicles. Additionally, considering the secondary indicators in B_1, the road lacks sidewalks and has incomplete sub-panels. Consequently, pedestrians face a higher risk on this road, necessitating focused efforts on pedestrian safety through diversion measures.

In the evaluation of M_3, C_{10} is classified as "Very poor," indicating a significant pedestrian flow on the road during peak hours. C_{11} ranks as "Excellent," signifying a considerably higher number of motorized vehicles than non-motorized vehicles within a unit of time. C_{12} falls under the "Poor" category, suggesting that pedestrians outnumber non-motorized vehicles passing the road within a given time frame. Therefore, it is evident that pedestrians and motorized vehicles are the primary participants in road traffic during peak hours. The deficiency in "Safety" is primarily manifested in the insufficient segregation of non-motorized lanes in C_3 and the occupation of pedestrian sidewalks by non-motorized vehicles in C_1. Hence, it is necessary to consider implementing segregation measures for non-motorized traffic to ensure safety.

Based on the analysis, the following diversion strategies around Xiangya Hospital can be recommended:

For M_1.

(1) Prohibit long-term parking of motor vehicles during peak hours and allow only temporary loading and unloading.
(2) Establish designated non-motorized parking areas in the front yard space of the hospital to free up pedestrian pathways from parking occupations.
(3) Designate a specific entrance for vehicles picking up and dropping off patients at the outpatient department, ensuring smooth traffic flow and convenience for patients arriving in private cars.

Fig. 9. "Safety" indicator evaluation results.

Fig. 10. "Accessibility" indicator evaluation results.

Fig. 11. "Traffic pressure" indicator evaluation results.

Fig. 12. "Convenience" indicator evaluation results.

Fig. 13. "Comfortableness" indicator evaluation results.

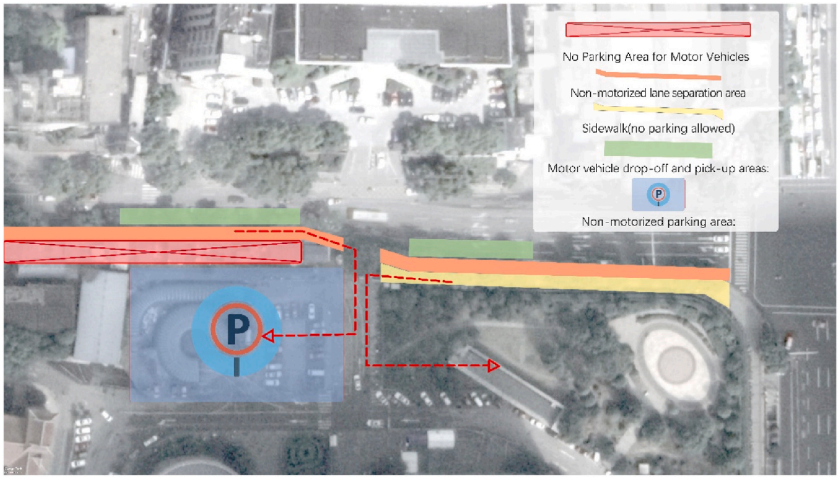

Fig. 14. Diversion strategies for M_1.

(4) Install temporary hard separation barriers to ensure the safety of pedestrians and cyclists (as Fig. 14 shows).

For M_3.

(1) Install separate and complete separation facilities for non-motorized vehicles from the intersection of Xiangya Road and Furong Middle Road.
(2) Ensure complete separation between non-motorized vehicles, motor vehicles, and pedestrians.
(3) Allow commuter cyclists to use the designated non-motorized vehicle facilities for seamless passage.
(4) Advise cyclists coming to the hospital to enter from Xiangya Road and utilize the parking lot established in front of the hospital for non-motorized vehicle parking.
(5) Implement this approach to address the issue of non-motorized vehicles occupying sidewalks near the hospital's outpatient department entrance.
(6) Install hard separation measures at the entrance of the outpatient department to restrict the intersection of vehicles and pedestrians (as Fig. 15 shows).

Analyzing the B_3 indicator for the N_1 reveals that C_{10} is rated as "Poor," indicating a high volume of pedestrian traffic during peak periods. Additionally, C_{12} is rated as "Moderate," suggesting a significant presence of non-motorized vehicles on the road during the same period. However, in the B_1 indicator, C_5 is rated as "Very poor," indicating the absence of a dedicated non-motorized lane on the road. Conversely, C_{11} is rated as "Good," indicating a low volume of motorized vehicles using the road during peak hours. Therefore, it is recommended to prioritize the establishment of a non-motorized lane to accommodate the high volume of pedestrian and non-motorized traffic on the N_1 road during peak hours.

In general, the road networks surrounding the two hospitals in Section N are deemed capable of ensuring fundamental safety standards in their present state, primarily owing to their high "Safety" ratings, although some of them perform poorly in the B_3 index during peak periods. The recommendation for the N_1 is to add a non-motorized lane with temporary hard separation facilities during the peak period.

Apart from the arterial roads encompassing the hospital, the nearby alleys are crucial in connecting vital traffic junctions and serving as essential routes for residents accessing the hospital. Specifically, these roads are M_9 to M_{14} and N_{11} to N_{20}. Unfortunately, owing to the outdated planning of the older city, these roads also show a series of conditions that need to be more friendly for pedestrians and cyclists.

Firstly, concerning the "Safety" indicators, only three are classified as "Good" or higher, while nine of them fall into the "Poor" or lower categories, exceeding half of the total. By analyzing the secondary indicators, it is evident that C_5 and C_6 have relatively lower ratings. Specifically, 15 samples from C_5 are categorized as "Very poor," while ten samples from C_6 are below the "Poor" category. This indicates that the most significant issue in the area is the inadequate provision of sidewalks and non-motorized paths.

Due to the substantial absence of sidewalks, it can be predicted that there is insufficient space to accommodate various barrier-free facilities. As a result, 15 roads in the sample are rated as "Very poor" for the "Accessibility" indicator. The main problem lies in the lack of tactile paving.

Regarding "Comfortableness," nine roads are rated as "Good" or higher, three are classified as "Moderate," and only four are labeled as "Poor" or below. The primary issues faced by roads with lower ratings are the inadequate provision of resting facilities (C_{19}) and shading (C_{20}).

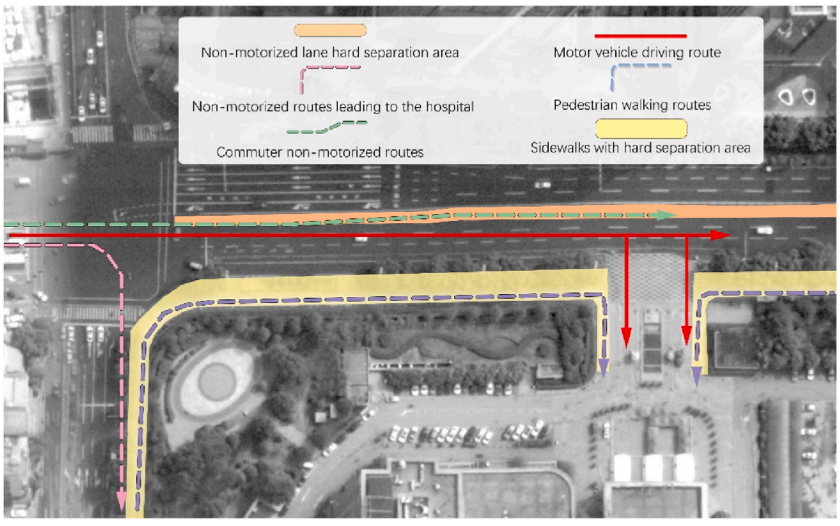

Fig. 15. Diversion strategies for M_3.

It is evident that pedestrian and cyclist safety has been overlooked in automobile-dominated urban designs, leading to the absence of sidewalks and non-motorized pathways. This oversight has further impacted the development of other essential infrastructure, such as tactile paving and street trees. On the one hand, it results in mixed traffic, where pedestrians, cyclists, and motor vehicles share the same roadway, thereby increasing safety hazards. On the other hand, it diminishes the appeal of the roads to active travel participants, failing to encourage people to adopt greener and healthier modes of travel. Therefore, such narrow lanes are recommended to restrict prolonged parking of motor vehicles and convert two-way lanes into one-way lanes. This would provide segregated safety spaces for pedestrians and cyclists, installing tactile paving, seating amenities for rest, and planting street trees to offer shade.

5. Conclusion

The arrival of the epidemic has given rise to many new urban problems. People began to pay attention to active travel and found that the city needs to provide a safe environment for pedestrians and cyclists in response to the new changes. Furthermore, traffic problems are especially prominent around large public buildings such as hospitals.

This study's significance lies in utilizing a novel model to assess and address the complex and hazardous traffic conditions surrounding large hospitals, particularly during public health crises such as COVID-19. It aims to evaluate the active travel space surrounding these hospitals and provide practical assessment and improvement strategies, offering theoretical insights for policymakers. Furthermore, it aims to optimize the travel experience for patients and other traffic participants while reducing accidents. Compared to previous studies, this research focuses on a more specific target. It proposes a more granular evaluation framework and methodology tailored to the current trend of active travel and the new changes in demands. Additionally, this study is grounded in the principles of Extenics theory. Unlike previous literature that solely assesses roads, it establishes a comprehensive logical chain from "identifying problematic roads" to "identifying the core issues" to "providing solutions," emphasizing the practical significance of addressing social issues through research.

However, there are certain areas for future improvement in the current study. To begin with, many factors may still affect the travel experience, such as noise and air quality. These street attributes could potentially impact pedestrians and non-motorized vehicle users' travel choices, subsequently affecting the evaluation outcomes. However, due to the random nature of such elements, such factors were not included in this study. Also, the weighting of comfort-related factors was minimal in the expert assignment and may not significantly impact the final results. Additionally, if a street is lengthy, there may be variations among different street segments in terms of facilities that impact pedestrian and cyclist travel behavior or safety. In other words, factors like road width or streetscape amenities may exhibit dynamic changes within a single street, thus influencing the assessment of the road. In this study, we have attempted to use a more reasonable calculation method to avoid errors. Moreover, due to the relatively consistent streetscape characteristics in the research area, we did not observe significant impacts on pedestrians and cyclists from differences in the street's ground-level interface during the survey and observation. Finally, in this study, the most representative hospital surroundings in the city center of Changsha were chosen as the research subject, encompassing various building functional types and a relatively well-organized road network. However, due to variations in urban planning and regional characteristics across different cities, the composition of building types or the configuration of road networks around hospitals may differ, the evaluation system may therefore need to be more deeply adapted to this type of situation. To address these concerns, in future research, we will strive to upgrade our research methods and evaluation indicators to develop a more detailed assessment model and indicator system.

Author contribution statement

Haoyu Deng: Conceived and designed the experiments; Performed the experiments; Wrote the paper. Tao Wang: Analyzed and interpreted the data; Contributed reagents, materials, analysis tools or data.

Data availability statement

Data included in article/supp. Material/referenced in article.

Declaration of competing interest

The authors declare that they have no known competing financial interests or personal relationships that could have appeared to influence the work reported in this paper.

Appendix A. Supplementary data

Supplementary data related to this article can be found at https://doi.org/10.1016/j.heliyon.2023.e19900.

References

[1] L. Hu, R.J. Schneider, Shifts between automobile, bus, and bicycle commuting in an urban setting, J. Urban Plann. Dev. 141 (2) (2015), https://doi.org/10.1061/(asce)up.1943-5444.0000214.

[2] S.D.S. Fraser, K. Lock, Cycling for transport and public health: a systematic review of the effect of the environment on cycling, Eur. J. Publ. Health 21 (6) (2010) 738–743, https://doi.org/10.1093/eurpub/ckq145.

[3] R. Hong, Z. Zhengtong, M. Xianrui, T. Xilai, Land use-slow traffic and demand forecasting, Open House Int. 42 (3) (2017) 130–134, https://doi.org/10.1108/ohi-03-2017-b0027.

[4] M. Cusack, Individual, social, and environmental factors associated with active transportation commuting during the COVID-19 pandemic, J. Transport Health 22 (2021), 101089, https://doi.org/10.1016/j.jth.2021.101089.

[5] S.S. Monfort, J.B. Cicchino, D. Patton, Weekday bicycle traffic and crash rates during the covid-19 pandemic, J. Transport Health 23 (2021), 101289, https://doi.org/10.1016/j.jth.2021.101289.

[6] J. Bert, D. Schellong, M. Hagenmaier, D. Hornstein, A.K. Wegscheider, T. Palme, How covid-19 will shape urban mobility (January 26), BCG Global, 2021. Retrieved January 11, 2023, from, https://www.bcg.com/publications/2020/how-covid-19-will-shape-urban-mobility.

[7] M. Ebrahim Shaik, S. Ahmed, An overview of the impact of covid-19 on road traffic safety and travel behavior, TRENG 9 (2022), 100119.

[8] A.I. Qureshi, W. Huang, S. Khan, I. Lobanova, F. Siddiq, C.R. Gomez, M.F. Suri, Mandated societal lockdown and road traffic accidents, ACCIDENT ANAL PREV 146 (2020), 105747.

[9] X. Yan, Z. Zhu, Quantifying the impact of covid-19 on E-bike safety in China via multi-output and clustering-based regression models, PLoS One 16 (8) (2021), https://doi.org/10.1371/journal.pone.0256610.

[10] A. Ramesh, P. Surpuriya, The value of a life: potentials and challenges for road safety of non-motorized transport users in Ahmedabad, Lecture Notes in Civil Engineering (2021) 215–230, https://doi.org/10.1007/978-981-33-4114-2_17.

[11] A. Nikitas, S. Tsigdinos, C. Karolemeas, E. Kourmpa, E. Bakogiannis, Cycling in the era of covid-19: lessons learnt and best practice policy recommendations for a more bike-centric future, Sustainability 13 (9) (2021) 4620, https://doi.org/10.3390/su13094620.

[12] C. Kyriakidis, I. Chatziioannou, F. Iliadis, A. Nikitas, E. Bakogiannis, Evaluating the public acceptance of sustainable mobility interventions responding to covid-19: the case of the Great Walk of athens and the importance of citizen engagement, Cities 132 (2023), 103966, https://doi.org/10.1016/j.cities.2022.103966.

[13] K. Teschke, M.A. Harris, C.C.O. Reynolds, M. Winters, S. Babul, M. Chipman, M.D. Cusimano, J.R. Brubacher, G. Hunte, S.M. Friedman, M. Monro, H. Shen, L. Vernich, P.A. Cripton, Route infrastructure and the risk of injuries to bicyclists: a case-crossover study, Am. J. Publ. Health 102 (12) (2012) 2336–2343, https://doi.org/10.2105/ajph.2012.300762.

[14] W. Wang, Z. Sun, L. Wang, S. Yu, J. Chen, Evaluation model for the level of service of shared-use paths based on traffic conflicts, Sustainability 12 (18) (2020) 7578, https://doi.org/10.3390/su12187578.

[15] R. Aldred, Motor traffic on Urban Minor and major roads: impacts on pedestrian and cyclist injuries, Proceedings of the Institution of Civil Engineers - Municipal Engineer 172 (1) (2019) 3–9, https://doi.org/10.1680/jmuen.16.00068.

[16] J.J. He, C.L. Jin, M. Cao, J.C. Wang, Z.W. Weng, Analysis on the parking problems of tertiary hospitals in the central urban area of Shanghai city, Chinese Hospital Management 35 (6) (2015) 27–28.

[17] J. Chen, Z. Li, H. Jiang, S. Zhu, W. Wang, Simulating the impacts of on-street vehicle parking on traffic operations on Urban Streets using cellular automation, Phys. Stat. Mech. Appl. 468 (2016) 880–891, https://doi.org/10.1016/j.physa.2016.11.060.

[18] D.S. Bai, P. Geng, Z.D. Wang, X.L. Wang, G.R. Xu, Q. Ye, N. Guo, Y. Zhao, C. Yang, H. Song, G.Q. Jiang, D.L. Xu, Practice and experience of regional medical center entrance linkage and closed-loop management under the wartime situation of the COVID-19 in China, 112, Ann. Transl. Med. 10 (2) (2022) 112, https://doi.org/10.21037/atm-22-61.

[19] Q. Wang, X. Wang, H. Lin, The role of triage in the Prevention and control of covid-19, Infect. Control Hosp. Epidemiol. 41 (7) (2020) 772–776, https://doi.org/10.1017/ice.2020.185.

[20] A.B. Teng, Z.B. Han, X.H. XuHongLi, J.F. JinFengFei, M.J. MingJuanAn, Evaluation system for pedestrian and bicycle transportation, Urban Transport of China 14 (5) (2016) 37–43, https://doi.org/10.13813/j.cn11-5141/u.2016.0505.

[21] J. Jin, K. Qi, M. Zhang, P.S. Qiao, Quantitative evaluation of walking accessibility in CBD——a case study of zhujiang new town in guangzhou and futian center in shenzhen, Chinese Landscape Architecture 8 (2016) 46–51.

[22] L.L. Guo, X.M. Tang, Evaluation of walking comfort of community roads under the background of city betterment and ecological restoration——a case of Shanghai caoyang new village, Chinese Landscape Architecture 36 (2020) 70–75, https://doi.org/10.19775/j.cla.2020.05.0070.

[23] X.X. Yan, Z.Z. Yuan, S.J. Mao, Y.L. Wu, Coordination evaluation of non-motorized traffic and urban design based on entropy weight—TOPSIS model, J. Highw. Transp. Res. Dev. 35 (9) (2018).

[24] Y. Liu, S. Chien, D. Hu, N. Wang, R. Zhang, (2020). Developing an extenics-based model for evaluating bus transit system, J. Adv. Transport. (2020) 1–13, https://doi.org/10.1155/2020/8879664.

[25] M. Cheng, W. Wei, (2020). An AHP-DEA approach of the bike-sharing spots selection problem in the free-floating bike-sharing system, Discrete Dynam Nat. Soc. (2020) 1–15, https://doi.org/10.1155/2020/7823971.

[26] C.Y. Yang, W. Cai, Extentics, China Science Publishing & Media Ltd., Beijing, China, 2014, pp. 5–6.

[27] J.M. Ling, H.C. Hao, L.X. Lu, Extension assessment method applying to pavement performance, J. Tongji Univ. 36 (1) (2008) 32–36.

[28] W. Cheng, M.R. Yuan, J.J. Zhao, Study on extenics evaluation of the safety for urban road intersections, Adv. Mater. Res. 779–780 (2013) 724–730. https://dx.doi.org/10.4028/www.scientific.net/amr.779-780.724.

[29] Y. Chen, J.X. Ma, Z.H. Xu, S.W. Qian, Research on evaluation method of bicycle traffic system based on matter element analysis, Forest Engineering 34 (5) (2018) 84–90.

[30] J. Eriksson, A. Niska, Å. Forsman, Injured cyclists with focus on single-bicycle crashes and differences in injury severity in Sweden, Accid. Anal. Prev. 165 (2022), 106510, https://doi.org/10.1016/j.aap.2021.106510.

[31] S. Chong, R. Poulos, J. Olivier, W.L. Watson, R. Grzebieta, Relative injury severity among vulnerable non-motorised road users: comparative analysis of injury arising from bicycle–motor vehicle and bicycle–pedestrian collisions, Accid. Anal. Prev. 42 (1) (2010) 290–296, https://doi.org/10.1016/j.aap.2009.08.006.

[32] J. Hong, D. McArthur, V. Raturi, Did safe cycling infrastructure still matter during a COVID-19 lockdown? Sustainability 12 (20) (2020) 8672, https://doi.org/10.3390/su12208672.

[33] Ministry of Housing and Urban-Rural Development, & China Acadamy of Urban Planning & Design, Planning Standards for Urban Pedestrian and Bicycle Transportation Systems (GB/T51439-2021)6–18, China Architectue Publishing & Media Co., Ltd, Beijing, China, 2021.

[34] S. Hu, H. Wu, H. Zhao, Annual China urban transportation planning conference 2016, Ser. Engineering Technology, in: Evaluation of Bicycle Traffic System Based on Hierarchical Entropy Analysis and Application Research vol. 2, Shenzhen; Beijing Municipal Engineering Design and Research Institute Co, 2016, pp. 1675–1683.

[35] Y. Ma, X. Gu, W. Zhang, S. Hu, H. Liu, J. Zhao, S. Chen, Evaluating the effectiveness of crosswalk tactile paving on street-crossing behavior: a field trial study for people with visual impairment, Accid. Anal. Prev. 163 (2021), 106420, https://doi.org/10.1016/j.aap.2021.106420.

[36] J.M. Barlow, A.C. Scott, B.L. Bentzen, D. Guth, J. Graham, Effectiveness of audible and tactile heading cues at complex intersections for pedestrians who are blind, Transport. Res. Rec.: J. Transport. Res. Board 2393 (1) (2013) 147–154, https://doi.org/10.3141/2393-17.

[37] F. Yuan, X. Ma, X. Xia, Prediction of slow city traffic demand based on space syntax, Forest Engineering 30 (6) (2014) 114–117, https://doi.org/10.16270/j.cnki.slgc.2014.06.020.
[38] N. Fagerholm, S. Eilola, V. Arki, Outdoor Recreation and nature's contribution to well-being in a pandemic situation - case Turku, Finland, Urban For. Urban Green. 64 (2021), 127257, https://doi.org/10.1016/j.ufug.2021.127257.
[39] E.H. Forman, S.I. Gass, The analytic Hierarchy process—an exposition, Oper. Res. 49 (4) (2001) 469–486, https://doi.org/10.1287/opre.49.4.469.11231.
[40] Office of the People's Government of Kaifu District, Overview of KaiFu distinctPeople's Government of Kaifu District，Changsha City (June 13), 2022. Retrieved October 26, 2022, from, http://www.kaifu.gov.cn/xingfukf/.
[41] T. Tian, Z.X. Li, The "Facebook" of representatives and members | How to put millions of electric bikes in Changsha?, January 7, 2020. Retrieved 26 October 2022, from, https://baijiahao.baidu.com/s?id=1655076164833444722&wfr=spider&for=pc.